



Contents lists available at ScienceDirect

## Arabian Journal of Chemistry

journal homepage: [www.ksu.edu.sa](http://www.ksu.edu.sa)

# The chemical profiling and identification of *Abelia macrotera* (Graebn. et Buchw.) Rehd. based on UHPLC-Q-Exactive Orbitrap MS and study their antioxidant, anti-tyrosinase and anti-inflammatory activities

Kaiquan Yu<sup>a,1</sup>, Jian Li<sup>a,1</sup>, Yuqi Chen<sup>a</sup>, Min Zhang<sup>a</sup>, Jiaxin Li<sup>a</sup>, Shani Li<sup>a</sup>, Qing Li<sup>a</sup>, Ling Liu<sup>a</sup>, Lilan Yi<sup>b,\*</sup>, Qingjiao He<sup>a,b,\*</sup>

<sup>a</sup> School of Pharmaceutical Sciences, Hunan University of Medicine, Huaihua 418000, China

<sup>b</sup> Hunan Provincial Key Laboratory of Dong Medicine, Hunan University of Medicine, Huaihua 418000, China

## ARTICLE INFO

## Keywords:

*Abelia macrotera*

UHPLC-Q-Exactive Orbitrap mass spectrometry

Phytochemical characterization

Antioxidant activity

Anti-inflammatory activity

## ABSTRACT

Although *Abelia macrotera* has long been used as the raw material for the special snack “immortal tofu” by Chinese population, the composition and activity of its leaf and stem are rarely studied. Ultrahigh-performance liquid chromatography-quadrupole (UHPLC-Q)-Exactive Orbitrap mass spectrometry and various experiments were used for *in vitro* study of its chemical composition and antioxidant, antityrosinase, and anti-inflammatory activities. A fast, accurate, and sensitive UHPLC-Q-Exactive Orbitrap mass spectrometry method has been established and effectively used for the determination of the chemical composition of the leaf and stem of *A. macrotera*. The biological activities of the leaf and stem extracts of the *A. macrotera* were determined *in vitro* by antioxidant and anti-inflammatory methods. A total of 142 chemical constituents including 48 flavonoids, 65 organic acids, 12 phenylpropanoids, and 19 others were identified by UHPLC-Q-Exactive Orbitrap mass spectrometry. The results show that the leaf and stem extracts have wide and significant antioxidant capacities, including scavenging effects of DPPH, ABTS and hydroxyl radicals, and the ability to reduce both iron and copper metal ions. Additionally, they showed a strong inhibition of NO production, with a dose-dependent inhibition. To the best of our knowledge, this is the first study to report the identification and content determination of the chemical components of the *A. macrotera* leaf and stem. These results will be beneficial to further understand its medicinal value.

## 1. Introduction

The *Abelia macrotera* (Graebn. et Buchw.) Rehd., also known as “shenxian tree” and “erchinuomitiao” in China, is a wild deciduous shrub plant of the genus *Abelia*, a family of the caprifoliaceae, which is primarily found in the Chinese provinces: Hunan, Shaanxi, Henan, Hubei, Sichuan, Guizhou and Yunnan (Committee, 2018). In ethnic regions, the leaf was widely used for food and medicine (Li et al., 2015). For example, the tender leaf was used for a famous food called “cold

jelly” in Dong nationality and the Wudang mountain area. The plant also has the effect of clearing heat and detoxification (Zhang, 2013). Previous investigations have shown that the *Abelia engleriana*, the plant of the same genus as *A. macrotera*, displayed several activities including antioxidant, anti-aging, anti-inflammatory, anti-tumor, and other effects (Duan et al., 2014).

Through chromatographic separation of *A. macrotera* in recent studies, a plethora of terpenoids and phenylpropanoids monomer compounds have been identified, demonstrating exceptionally potent anti-

**Abbreviations:** Absb, Background absorbance; Absc, Control absorbance; Abss, Sample absorbance; CD, Compound Discovery; CUPRAC, copper ions reducing antioxidant power; EIC, extracted ion chromatograms; ESI, electrospray ionization source; FRAP, ferric iron reducing antioxidant power; MS, mass spectrometry; OTCML, the Orbitrap Traditional Chinese Medicine Library; PRM, parallel reaction monitoring; TCM, traditional Chinese medicine; UHPLC-MS/MS UHPLC-Q-Exactive Orbitrap MS, ultra-performance liquid chromatography-quadrupole-electrostatic field Orbitrap mass spectrometry.

Peer review under responsibility of King Saud University.

\* Corresponding authors.

E-mail addresses: [girlying5200@163.com](mailto:girlying5200@163.com) (L. Yi), [jj702@163.com](mailto:jj702@163.com) (Q. He).

<sup>1</sup> K. Yu and J. Li contributed equally to this work.

<https://doi.org/10.1016/j.arabjc.2023.105575>

Received 15 October 2023; Accepted 16 December 2023

Available online 20 December 2023

1878-5352/© 2023 The Author(s). Published by Elsevier B.V. on behalf of King Saud University. This is an open access article under the CC BY-NC-ND license (<http://creativecommons.org/licenses/by-nc-nd/4.0/>).

inflammatory activity. Additionally, it was discovered that these compounds exert a significant inhibitory effect on NO production in lipopolysaccharide (LPS)-induced RAW264.7 cells (Xu et al., 2022). However, studies have focused on the chemical and biological activities of *A. macrotera*. Therefore, it is necessary to elucidate the chemical composition as well as the physiological activity of this compound.

Ultra-high performance liquid chromatography-mass spectrometry (UHPLC-MS/MS) has been developed as a highly sensitive and powerful instrument over the past few years, which provides precise information on ion precursors and fragment ions from MS/MS. This is beneficial for improving the authenticity of the characterization of small and medium-sized molecules in mixtures (Bai et al., 2020). To determine which species are responsible for the nutritional effects of *A. macrotera*, our study examined the chemical composition of the leaf and stem using the UHPLC-Q-Exactive Orbitrap MS with multiple data mining.

Many detrimental health effects have been linked to free radicals, including aging, diabetes, cardiovascular disease, and neurodegenerative disorders (Lee et al., 2020). As reported by previous studies, phenolic compounds (such as flavonoids, anthocyanins and phenolic acids) possess good antioxidant activity (Zhang et al., 2023) and play a crucial role in the prevention of chronic diseases (Delgado et al., 2019). In light of the potential carcinogenic and toxic effects of synthetic antioxidants, natural antioxidants have been suggested to be safer and healthier alternatives for use in food. Therefore, the mechanism of natural antioxidants has attracted considerable attention, especially in the treatment of diabetes (Sun et al., 2021). The literature has shown that natural antioxidants have a wide range of uses, for example, *Achillea pseudoaleppica*, a type of natural medicine, offers promising antioxidant properties (Yilmaz et al., 2023), and *Satureja boissieri*, which has been proven to have high antiradical, antioxidant activity, can be used as an alternative for antibiotics (Aras et al., 2018).

Present study involves both qualitative and quantitative evaluation of *A. macrotera*, aiming to establish a reference for assessing its quality and a scientific foundation for comprehending its pharmacological effects. *In vitro* characterizations were performed, including UHPLC-Q-Exactive Orbitrap MS, to understand the chemical composition and antioxidant, antityrosinase, and anti-inflammatory activities, which play a significant role in the characterization results established the quality control and the nutritional ingredient for research. This method will serve as a benchmark to establish quality standards, as well as for the development and utilization of *A. macrotera* in the future.

## 2. Materials and methods

### 2.1. Materials and reagents

Supplementary Table S1 provides detailed information about the reference standard substances. Formic acid was obtained from Fisher Scientific (New Jersey, USA) as LC-MS grade. Chromatographic grade methanol and acetonitrile were provided by Merck KGaA (New Jersey America). A Milli-Q system (Millipore, Milford, MA, USA) was used to purify deionized water. From TCI (Shanghai) Development Co., Ltd, 1,1-Diphenyl-2-picrylhydrazyl Free Radicals (DPPH) were purchased. 2,2'-Azinobis(3-ethylbenzthiazoline-6-sulphonate) (TPTZ), levodopa and Fetal bovine serum was purchased from Shanghai Yuanye Biotechnology Co., Ltd. L-ascorbic acid (AR) and Potassium persulfate (AR) were purchased from Sinopharm Chemical Reagent Co., Ltd. Salicylic acid and Iron sulfate heptahydrate were obtained from Aladdin Biochemical Technology Co., Ltd. (Shanghai). 3-(4,5-Dimethylthiazol-2-yl)-2,5-diphenyltetrazolium bromide (MTT) was purchased from Sangon Biotech (Shanghai) Co., Ltd., Nitric Oxide Assay Kit was purchased from Beyotime Biotechnology (Shanghai) Co., Ltd. Other chemicals and solvents used in this study were of analytical grade.

### 2.2. Plant materials

The plant materials used in this study were collected from Shaoyang, Hunan Province, China in July 2021 and identified as the leaves and stems of *Abelia macrotera* (Graebn. et Buchw.) Rehd. by Professor W. Cai of the Hunan University of Medicine.

#### 2.2.1. Preparation of the plant materials and extracts

Freshly harvested stem of *A. macrotera* was meticulously separated from its leaf, followed by precise segmentation into small, uniform pieces. The leaf and stem of the *A. macrotera* were dried in an oven at a temperature of 55 °C and pulverized and sieved (60 mesh) (Zhang, 2013). The resulting plant material was stored in a dry environment.

A total of 1.0 kg of samples were sonicated (Ultrasonic cleaner, 300 w) for 1 h with 70 % methanol at (1:15 w/v) at temperature of 25 °C, and the extracts were filtrated. The obtained extract was subjected to reflux using a rotary evaporator, with methanol being evaporated to yield a concentrated solution. Using the LGJ-10C vacuum freeze dryer (Sihuan Furuikeyi Technology Development Co., Ltd.), the liquid was condensed and frozen dried, to obtain 116.3 g of leaf extract and 111.0 g of stem extract of *A. macrotera*. Finally, the lyophilized extract was stored at -20 °C for further investigation.

#### 2.3. Assay of total polysaccharides, flavonoids, and polyphenols

The content of polysaccharide, flavonoid, and polyphenol were determined by the phenol-sulfuric acid method, the sodium nitrite-aluminum nitrate-sodium hydroxide method, and the sodium nitrite-aluminum nitrate-sodium hydroxide method with d-glucose, rutin, and gallic acid as the standards, respectively. Triplicate analyses were conducted in all cases.

#### 2.4. UPLC-Q-Exactive Orbitrap MS analyses

##### 2.4.1. Preparation of standard solutions

A single standard (20 mg/mL) was accurately weighed to prepare a stock solution and dissolved in 1 mg/mL methanol. To conduct further analysis, a mixed standard was prepared by mixing 30 individual standard solutions. The resulting mixed standard was then diluted with methanol to achieve a concentration of 2 mg/mL and stored at -20 °C.

##### 2.4.2. Preparation of sample

To prepare the sample, 1 mg of the leaf and stem extract of *A. macrotera* was dissolved in 1 mL of methanol and centrifuged at 12,000 r/min for 15 min at 4 °C. The upper solution was filtered using a 0.22 µm millipore filter and stored at -20 °C before injection into the UHPLC-HRMS.

##### 2.4.3. Instrumentation and UHPLC-MS/MS conditions

UHPLC analyses were completed using an Ultimate 3000 (Dionex, Sunnyvale, CA, USA) system. Samples were separated at 40 °C using a Thermo Scientific Hypersil GOLD aQ (100 × 2.1 mm, 1.9 µm). The injection volume of the samples was 2 µL. The flow rate was set at 0.30 mL/min. The mobile phase consisted of 0.1 % of formic acid in water (A) and acetonitrile (B), with optimized gradient elution conditions of: 0–2 min, 5–10 % B; 2–5 min, 10–20 % B; 5–10 min, 20–25 % B; 10–12 min, 25–55 % B; 12–20 min, 55–80 % B; 20–25 min, 80–95 % B; 25–26 min, 95–5 % B; 26–30 min, 5 % B.

The UHPLC system was outfitted with a Q-Exactive Orbitrap MS (Thermo Fisher Scientific, Bremen, Germany), this instrument was equipped with a heated electrospray ionization source (HESI) capable of scanning in negative and positive modes between  $m/z$  120 and 1000. The key parameters were as follows: for (-)-ESI and (+)-ESI, the ion spray voltage was 3.0 and 3.5 kV, respectively, and for sheath and auxiliary gas it was one and 10 arbitrary units, respectively. The temperature of the capillary and the auxiliary gas heaters were maintained

at 320 and 350 °C, respectively. The MS<sup>1</sup> spectra were acquired with full MS mode at a resolution of 35,000 and MS<sup>2</sup> spectrum with the top 3 ions' MS/MS fragmentation (dd-MS<sup>2</sup>-TOP3) or parallel reaction monitoring mode at a resolution of 17,500. For MS/MS acquisitions, the NCE (normalized collision energy) was 30 %.

#### 2.4.4. Data processing and analysis

A combination of Xcalibur 4.2 software and Compound Discovery 3.0 software (Thermo Fisher Scientific, California, USA) was used for the acquisition and analysis of the data. In the CD software, the raw LC-MS data were imported by using a TCM workflow, consisting of mzvault, mzcloud, and the Orbitrap Traditional Chinese Medicine Library (OTCML). The TCM workflow template was optimized with the following parameters: MS<sup>1</sup> and MS<sup>2</sup> with mass tolerances of 10 ppm, the retention time limit of 0.5–28 min, the maximum element counts of C<sub>60</sub>H<sub>60</sub>O<sub>60</sub>N<sub>10</sub>, the minimum peak intensity of 1,000,000 and the S/N threshold of 10. The data processing software of Compound Discoverer 3.1 was used to perform peak matching and peak area extraction on the original data from the primary mass spectrometry.

### 2.5. Antioxidant activity assays

#### 2.5.1. DPPH radical scavenging activity

The DPPH free radical scavenging was determined according to the previously reported method (Zong et al., 2021). Briefly, 1 mL of different concentrations (0.0025, 0.005, 0.01, 0.025, 0.05, 0.1 and 0.15 mg/mL) of the leaf and stem extracts were mixed with 1 mL of a DPPH ethanol solution (0.2 mM) in a test tube. The background group used ethanol instead of the DPPH solution, and the control group used ethanol instead of the sample solution. Ascorbate was used as a positive control. After 30 min of incubation in the dark at 37 °C, a 200 µL aliquot was taken and placed in a 96-microwell detector, and the absorbance was measured at 517 nm using a multifunctional microplate reader (BMG LABTECH, Germany). All determinations were performed in triplicate. The DPPH radical scavenging activity was calculated as follows:

$$\text{DPPHradicalscavengingactivity}(\%) = \left(1 - \frac{(\text{Abss} - \text{Absb})}{\text{Absc}}\right) \times 100\%$$

Where Abss, Absc and Absb correspond to the sample, control, and background absorbances, respectively.

#### 2.5.2. ABTS radical scavenging activity

A previously reported method was used to determine the free radical scavenging capability of ABTS (Kuppusamy et al., 2015). Briefly, a total of 1 mL of different concentrations (0.005, 0.01, 0.025, 0.05, 0.1 and 0.15 mg/mL) of the leaf and stem extracts were mixed with 2 mL of an ABTS solution in a test tube. The background group used purified water instead of the ABTS solution, and the control group used purified water instead of the sample solution. Ascorbic acid was used as a positive control. The solutions were incubated for 6–8 min at 37 °C without light, after which a 200 µL aliquot was removed and placed in a 96-microwell detector. The absorbance at 734 nm was determined using a multi-function microplate reader. All determinations were performed in triplicate. The ABTS radical scavenging activity was determined as follows:

$$\text{ABTSradicalscavengingactivity}(\%) = \left(1 - \frac{(\text{Abss} - \text{Absb})}{\text{Absc}}\right) \times 100\%$$

Where Abss, Absc and Absb correspond to the sample, control, and background absorbances, respectively.

#### 2.5.3. •OH radical scavenging activity

The hydroxyl radical scavenging activity was evaluated by the salicylate method, with slight modifications to that previously reported (Zong et al., 2021). Briefly, the leaf and stem extract were separately diluted to a concentration (0.0625, 0.125, 0.25, 0.5 and 1.0 mg/mL) using pure water as the solvent. Then 25 µL of ferrous sulfate (9 mmol/L), 0.03 % hydrogen peroxide, and salicylate-ethanol solution (9 mmol/L) were each mixed with a 125 µL aliquot of different sample solution in a 96-microwell detector. The background group used purified water instead of the 0.03 % hydrogen peroxide, and the control group used purified water instead of the sample solution. Positive control was provided by ascorbic acid. Under dark conditions, the mixture was heated to 37 °C for 30 min, and the absorbance at 510 nm was determined using a multi-function microplate reader. All experiments were performed in triplicate and the ABTS radical scavenging activity was calculated as follows:

Where Abss, Absc and Absb correspond to the sample, control, and background absorbances, respectively.

$$\cdot\text{OHradicalscavengingactivity}(\%) = \left(1 - \frac{(\text{Abss} - \text{Absb})}{\text{Absc}}\right) \times 100\%$$

Where Abss, Absc and Absb correspond to the sample, control, and background absorbances, respectively.

#### 2.5.4. FRAP and CUPRAC/antioxidant capacity assays for the reduction of transition metal ions

The ferric reducing ability of plasma (FRAP) assay was determined according to the previously reported method (Masek et al., 2020) with slight modifications, which involved the reduction of Fe<sup>3+</sup> to Fe<sup>2+</sup>. The FRAP reagent consisted of acetate buffer (300 mM, pH 3.6), ferric chloride (20 mM), and a solution of 10 mM 2,4,6-tripyridyl-s-triazine (TPTZ) in hydrochloric acid (40 mM) at the ratio of 10:1:1 (v/v/v). A total of 20 µL of different concentrations (0.0625, 0.125, 0.25, 0.5, 1.0 and 2.0 mg/mL) of the leaf and stem extracts were mixed with 180 µL of the FRAP reagent in a 96-well plate and incubated for 5 min at 25 °C in the dark. The background group used purified water instead of the sample solution. The absorbance at 593 nm was determined using a multi-function microplate reader. Ferrous sulfate (FeSO<sub>4</sub>·7H<sub>2</sub>O) was used to develop a 0.05–1.6 µmol/L standard curve. All results were expressed as Fe<sup>2+</sup> content (Fe<sup>2+</sup> mmol/L). A triplicate of each test was performed.

The cupric reducing antioxidant capacity (CUPRAC) assay was determined using the previously reported method with slight modifications (Han et al., 2012), which involved the reduction of Cu<sup>2+</sup> to Cu<sup>+</sup>. A 60 µL aliquot of CuSO<sub>4</sub> (0.01 M) was mixed with 60 µL of an ethanol solution of neocuproine (7.5 mM) and 60 µL of a buffer solution CH<sub>3</sub>COONH<sub>4</sub> (1 M) in a 96-microwell detector, followed by the addition of different concentrations (0.125, 0.25, 0.5, 1.0 and 2.0 mg/mL) of the leaf and stem extracts. The background group used purified water instead of the sample solution. After 30 min of incubation at 25 °C in the dark, the absorbance at 450 nm was determined using a multi-function microplate reader. CUPRAC was defined as:

$$\Delta A = A_1 - A_0$$

Where A<sub>0</sub> is the absorbance of the reagent test, and A<sub>1</sub> is the absorbance of the sample.

### 2.6. In vitro tyrosinase inhibitory assay

The tyrosinase inhibitory ability of the leaf and stem extracts were examined in vitro using levodopa as a substrate, a slightly modified method compared with that previously described (Klomsakul et al., 2022). Tyrosinase and levodopa were diluted in PBS (0.02 M, pH 6.8) to 250 U/mL and 2.5 mM, respectively. A 40 µL aliquot of extracts at different concentrations (0.03125–2 mg/mL) was combined with 40 µL of tyrosinase solution and 80 µL of 0.02 M of PBS (pH 6.8) solution. The resultant solution was evenly mixed, and incubated at 25 °C for 20 min. The reaction was mixed by adding 40 µL of the levodopa solution and incubated at 25 °C for 10 min. Finally, the absorbance was measured at 475 nm using a multi-function microplate reader. Vitamin C (Vc) was used as a positive control, the sample background group did not contain levodopa, the control group used PBS instead of the sample extracts, and the blank group contained no sample and levodopa. Experiments were

performed in triplicate. The inhibition rate of the tyrosinase activity was calculated as follows:

$$\text{Tyrosinase inhibition}(\%) = \left(1 - \frac{(A - B)}{(C - D)}\right) \times 100\%$$

Where A is absorbance of the sample; B is the absorbance of the sample background; C is the absorbance of the control group; and D is the blank group.

## 2.7. Cell experiments to determine anti-inflammatory ability

### 2.7.1. Cell culture

The Cell Bank of Chinese Academy of Sciences (Shanghai) provided the macrophage-like cell line RAW264.7. The culture medium was high-glucose Dulbecco's modified Eagle medium (DMEM), with 10 % heat-inactivated FBS and 1 % penicillin. Cells were grown at 37 °C in a humidified incubator with 5 % CO<sub>2</sub>. Cells in the log growth cycle were selected for the experiments. The cells used for the experiments were all in the fourth to fifteenth passages. Cells were fluid-changed on the day before inoculation.

### 2.7.2. Cell viability assay

The cells seeded in a 96-well plate ( $5 \times 10^4$  cells/mL) were divided into either the blank, control, or drug groups (0.1, 0.2, 0.4 mg/mL). First, RAW264.7 cells were treated with the respective concentrations of the drug solutions (100 μL) for 24 h. Then, 10 μL of MTT (5 mg/mL) solution was added to each well, except for the blank group. Subsequently, the cells were placed in an incubator for a further 4 h incubation. Finally, the absorbance at 490 nm was measured using a multifunctional microplate reader after 100 μL of DMSO solution was added to each well and mixed for 10 min. The cell viability was calculated as follows:

$$\text{Cell viability}(\%) = \frac{(\text{OD sample group} - \text{OD blank group})}{(\text{OD control group} - \text{OD blank group})} \times 100\%$$

### 2.7.3. NO concentration assay

RAW264.7 cells ( $3 \times 10^5$  cells/mL) were placed in a 96-well plate and grown for 24 h until the cells were completely adherent. cells were treated with DEX (1 μM) and the leaf and stem extracts (0.1, 0.2, and 0.4 μg/mL). After 1 h, LPS (0.1 μg/mL) was added to treat the cells for 18 h. The supernatant was collected and mixed with 100 μL of Griess reagent, then the absorbance was measured at 540 nm, according to the requirements of the NO detection kit (Beyotime, Shanghai, China). The absorbance was measured on a multi-function microplate reader at the wavelength of 540 nm. The concentration of NO was then calculated from the standard curve. All of the tests were measured in triplicate.

## 2.8. Statistical analysis

All the tests were conducted in triplicate, and the results presented the average of the analyses and stated as mean ± SD. Analyses were conducted using GraphPad Prism software (GraphPad Prism version 9, San Diego, CA, USA). The statistical significance differences between two groups and multiple groups were calculated by one-way analysis of variance (ANOVA) and Dunnett's Multiple Comparison Test, and the statistical significance was determined when  $P < 0.05$ .

## 3. Results and discussion

### 3.1. Chemical contents of *A. macrotera*

Among the extract of the leaf, polysaccharides (55 %) were found along with polyphenols (35 %), and flavonoids (22 %). The stem extract was composed of polysaccharides (35 %), polyphenols (20 %), and flavonoids (9 %). Some studies show that polysaccharides have anti-

inflammatory activities, antioxidant activities, and analgesic effects (Hou et al., 2020), while polyphenols present in plants have antioxidant capacity (Aras et al., 2018). Thus, the antioxidant and anti-inflammatory activities of *A. macrotera* may be mediated by polysaccharides and polyphenols.

### 3.2. Identification of chemical constituents in leaf and stem

As shown in Table 1, a total of 142 and 104 compounds are determined in the leaf and stem (Fig. 1) of *A. macrotera*, respectively, including 48 kinds of flavonoids, 65 organic acids, 11 phenylpropanoids and 18 others (comprehensive information appears in Supplementary Material Table S2). This data highlights that there is an abundance of chemical components in *A. macrotera*. The extracted ion chromatograms (EICs) of these compounds in both positive and negative ion modes are shown in Fig. 2.

#### 3.2.1. Identification of flavonoids and derivatives

A total of 48 flavonoids were preliminarily identified in *A. macrotera*. The peaks obtained from mass spectrum at 56, 94, 96, 97, 98, 102, 105, 121, 125, 130, and 132 were accurately identified as catechin, rutin, quercetin, isoquercitrin, kaempferol-3-O-neohesperidoside, luteoloside, kaempferol-7-O-glucoside, eriodictyol, luteolin, kaempferol, and isorhamnetin based on the retention time and MS<sup>2</sup> pattern of the corresponding reference standard.

The peak 45, with [M-H]<sup>-</sup> ion at  $m/z$  451.1246, could be characterized as catechin-glucopyranoside, which produced some characteristic fragment ions at  $m/z$  289.0714 [M-H-C<sub>6</sub>H<sub>10</sub>O<sub>5</sub>]<sup>-</sup>, 205.0497, and 137.0231. Peak 67 showed a precursor ion at  $m/z$  625.1410 [M-H]<sup>-</sup> and was suggested to be quercetin-dihexoside based on the product ions at  $m/z$  463.0885 [M-H-C<sub>6</sub>H<sub>10</sub>O<sub>5</sub>]<sup>-</sup> and 301.0348 [M-H-2C<sub>6</sub>H<sub>10</sub>O<sub>5</sub>]<sup>-</sup>, in line with the literature characterization (Sánchez-Salcedo et al., 2016). Peaks 81 and 88 possessed the same parent ion at  $m/z$  755.2040 and produced product ions at  $m/z$  301.0334, 178.9977 and 151.0029, therefore, they were attributed to quercetin rutin rhamnoside. Peak 84 displayed a [M-H]<sup>-</sup> ion at  $m/z$  595.1305 and yielded a fragment ion at  $m/z$  301.0347 [M-H-C<sub>6</sub>H<sub>10</sub>O<sub>5</sub>-C<sub>5</sub>H<sub>8</sub>O<sub>4</sub>]<sup>-</sup>, which corresponded to the loss of a glucose and an arabinose moiety. Thus, peak 84 was tentatively identified as quercetin-arabinosylglucoside based on literature research (Zeng et al., 2017). Peak 106, with a parent ion [M-H]<sup>-</sup> at  $m/z$  433.0776, was identified as quercetin-pentoside due to the fragment ion at  $m/z$  301.0338 [M-H-C<sub>5</sub>H<sub>8</sub>O<sub>4</sub>]<sup>-</sup> and 271.0237 [M-H-C<sub>5</sub>H<sub>8</sub>O<sub>4</sub>-CO-2H]<sup>-</sup>, which were related to the loss of xylan.

Peaks 71, 79, 83, 86, 110, 112, 117, 137 and 140 were respectively characterized as vicenin II, schaftoside, isoschaftoside, eriocitrin, rhoifolin, narcissoside, neodiosmin, demethylnobletin and demethylnobletin isomer, when compared with the mzVault.

Peaks 70, 80, and 90 possessed the same precursor ion [M-H]<sup>-</sup> at  $m/z$  449.1089, which loses a molecule of rhamnose to produce  $m/z$  285.0404 [M-H-C<sub>6</sub>H<sub>10</sub>O<sub>5</sub>-2H]<sup>-</sup>, and loses another molecule to produce the quercetin characteristic ion at  $m/z$  125.0232 [M-H-2C<sub>6</sub>H<sub>10</sub>O<sub>5</sub>]<sup>-</sup>, thus they were identified as the taxifolin-7-rhamnoside isomer. Compared with the literature, peak 114 and peak 126 were identified as ashesperetin or the hesperetin isomer, peak 123 was characterized as calycosin, peak 131 and peak 133 were identified as chrysoeriol or the chrysoeriol isomer, and peak 134 was identified as genkwanin (Vieira de Moraes et al., 2021).

Among the 48 kinds of flavonoids and their derivatives in the characterization, 48 were found in the leaf, while only 32 compounds were found in the stem. The leaf-specific compounds included taxifolin-7-rhamnoside, quercetin-rhamnosyl rutin, isorhamnetin-3-O-neohesperidine, and rhoifolin, which indicates that the biological activity of the leaf may be better than that of the stem. Thus, *A. macrotera* proved to be a promising source of flavonoids that may have valuable applications in the medical, healthcare, food, and pharmaceutical industries.

**Table 1**  
Identification of 142 chemical constituents in *A. macrotera* by UHPLC-Q-Exactive Orbitrap MS.

Peak	t <sub>R</sub>	Theoretical Mass m/z	Experimental Mass m/z	Error (ppm)	Formula	Identification/ Reactions	source	Peak	t <sub>R</sub>	Theoretical Mass m/z	Experimental Mass m/z	Error (ppm)	Formula	Identification/Reactions	source
1	0.85*	191.05611	191.05518	-4.87	C <sub>7</sub> H <sub>12</sub> O <sub>6</sub>	Quinic acid	L	72	5.89	167.03498	167.03392	-6.36	C <sub>8</sub> H <sub>8</sub> O <sub>4</sub>	4-Methoxysalicylic acid	L
							S								S
2	0.88	175.11895	175.11853	-2.41	C <sub>6</sub> H <sub>14</sub> N <sub>4</sub> O <sub>2</sub>	Arginine	L	73	5.89	355.10345	355.10327	-0.52	C <sub>16</sub> H <sub>20</sub> O <sub>9</sub>	Ferulic Acid-hexoside	L
							S								S
3	0.91	195.05102	195.05013	-4.59	C <sub>6</sub> H <sub>12</sub> O <sub>7</sub>	Gluconic acid	L	74	5.96	175.02481	175.02383	-5.61	C <sub>6</sub> H <sub>8</sub> O <sub>6</sub>	Ascorbic acid isomer	L
							S								
4	0.91	341.10893	341.10855	-1.13	C <sub>12</sub> H <sub>22</sub> O <sub>11</sub>	Sucrose	L	75	5.98	415.16097	415.15945	-3.66	C <sub>19</sub> H <sub>28</sub> O <sub>10</sub>	Phenylethanol rutin	L
							S								
5	0.94	193.03537	193.03453	-4.38	C <sub>6</sub> H <sub>10</sub> O <sub>7</sub>	D-Galacturonic acid	L	76	6.26*	163.04007	163.03893	-6.98	C <sub>9</sub> H <sub>8</sub> O <sub>3</sub>	4-Coumaric acid	L
							S								
6	0.94	209.03029	209.02951	-3.73	C <sub>6</sub> H <sub>10</sub> O <sub>8</sub>	Saccharic acid	L	77	6.28	415.16097	415.16110	0.31	C <sub>19</sub> H <sub>28</sub> O <sub>10</sub>	Phenylethanol rutin	L
							S								
7	0.95	148.06043	148.06013	-2.05	C <sub>5</sub> H <sub>9</sub> NO <sub>4</sub>	L-Glutamic acid	L	78	6.28*	173.08193	173.08095	-5.67	C <sub>8</sub> H <sub>14</sub> O <sub>4</sub>	Suberic acid	L
							S								
8	0.97	138.05496	138.05469	-1.92	C <sub>7</sub> H <sub>7</sub> NO <sub>2</sub>	Trigonelline	L	79	6.33	563.14062	563.14032	-0.55	C <sub>26</sub> H <sub>28</sub> O <sub>14</sub>	Schaftoside	L
							S								
9	0.98*	133.01425	133.01302	-9.22	C <sub>4</sub> H <sub>6</sub> O <sub>5</sub>	Malic acid	L	80	6.52	449.10893	449.10858	-0.79	C <sub>21</sub> H <sub>22</sub> O <sub>11</sub>	Taxifolin 7-rhamnoside	L
							S								
10	1.00*	145.01425	145.01311	-7.84	C <sub>5</sub> H <sub>6</sub> O <sub>5</sub>	α-Ketoglutaric acid	L	81	6.63	755.20402	755.20392	-0.13	C <sub>33</sub> H <sub>40</sub> O <sub>20</sub>	Quercetin rutin rhamnoside	L
							S								
11	1.00	173.00916	173.00815	-5.84	C <sub>6</sub> H <sub>6</sub> O <sub>6</sub>	Trans-Aconitic acid	L	82	6.74	173.08193	173.08110	-4.81	C <sub>8</sub> H <sub>14</sub> O <sub>4</sub>	Suberic acid isomer	L
12	1.00	175.02481	175.02382	-5.66	C <sub>6</sub> H <sub>8</sub> O <sub>6</sub>	Ascorbic acid	L	83	6.88	563.14062	563.14038	-0.44	C <sub>26</sub> H <sub>28</sub> O <sub>14</sub>	Isoschaftoside	L
							S								
13	1.00*	191.01973	191.01880	-4.85	C <sub>6</sub> H <sub>8</sub> O <sub>7</sub>	Citric acid	L	84	6.88	595.13046	595.12866	-3.02	C <sub>26</sub> H <sub>28</sub> O <sub>16</sub>	quercetin-arabinosylglucoside	L
							S								
14	1.03	149.00916	149.00769	-9.87	C <sub>4</sub> H <sub>6</sub> O <sub>6</sub>	Tartaric acid	L	85	6.90*	193.05063	193.04959	-5.40	C <sub>10</sub> H <sub>10</sub> O <sub>4</sub>	Ferulic acid	L
							S								
15	1.19*	129.01933	129.01814	-9.24	C <sub>5</sub> H <sub>6</sub> O <sub>4</sub>	Citraconic acid	L	86	6.93	595.16684	595.16760	1.27	C <sub>27</sub> H <sub>32</sub> O <sub>15</sub>	Eriocitrin	L
							S								
16	1.19*	173.00916	173.00822	-5.44	C <sub>6</sub> H <sub>6</sub> O <sub>6</sub>	Cis-aconitic acid	L	87	6.95	609.14611	609.14612	0.02	C <sub>27</sub> H <sub>30</sub> O <sub>16</sub>	Rutin isomer	L
							S								
17	1.20	123.05529	123.05522	-0.56	C <sub>6</sub> H <sub>6</sub> N <sub>2</sub> O	Nicotinamide	L	88	6.95	755.20402	755.20361	-0.54	C <sub>33</sub> H <sub>40</sub> O <sub>20</sub>	Quercetin rutin rhamnoside	L
							S								
18	1.22	182.08116	182.08084	-1.81	C <sub>9</sub> H <sub>11</sub> NO <sub>3</sub>	L- Tyrosine	L	89	7.06	639.19306	639.19299	-0.11	C <sub>29</sub> H <sub>36</sub> O <sub>16</sub>	β-Hydroxyverbascoside	L
							S								
19	1.32	147.06628	147.06526	-6.95	C <sub>6</sub> H <sub>12</sub> O <sub>4</sub>	Mevalonic acid	L	90	7.11	449.10893	449.10831	-1.39	C <sub>21</sub> H <sub>22</sub> O <sub>11</sub>	Taxifolin 7-rhamnoside	L
							S								
20	1.32	191.05611	191.05516	-4.98	C <sub>7</sub> H <sub>12</sub> O <sub>6</sub>	Quinic acid isomer	L	91	7.18	217.10814	217.10744	-3.26	C <sub>10</sub> H <sub>18</sub> O <sub>5</sub>	Epieucommiol	L
							S								
21	1.56*	169.01425	169.01338	-5.13	C <sub>7</sub> H <sub>6</sub> O <sub>5</sub>	Gallic acid	L	92	7.26	181.04954	181.04918	-1.96	C <sub>9</sub> H <sub>8</sub> O <sub>4</sub>	Caffeic acid isomer	L
22	1.66	331.06707	331.06720	0.39	C <sub>13</sub> H <sub>16</sub> O <sub>10</sub>	Monogalloyl-glucose	L	93	7.29*	137.02442	137.02322	-8.74	C <sub>7</sub> H <sub>6</sub> O <sub>3</sub>	Salicylic acid	L
							S								
23	1.73	315.07216	315.07187	-0.90	C <sub>13</sub> H <sub>16</sub> O <sub>9</sub>	Protocatechuic acid-O-glucoside	L	94	7.29*	609.14611	609.14594	-0.28	C <sub>27</sub> H <sub>30</sub> O <sub>16</sub>	Rutin	L
							S								
24	1.83	373.11402	373.11404	0.05	C <sub>16</sub> H <sub>22</sub> O <sub>10</sub>	Geniposidic acid	L	95	7.34	623.19814	623.19812	-0.04	C <sub>29</sub> H <sub>36</sub> O <sub>15</sub>	Verbascoside	L
							S								
25	1.85	164.07170	164.07072	-5.98	C <sub>9</sub> H <sub>11</sub> NO <sub>2</sub>	L-Phenylalanine	L	96	7.40*	301.03537	301.03482	-1.85	C <sub>15</sub> H <sub>10</sub> O <sub>7</sub>	Quercetin	L
							S								
26	2.02	218.10339	218.10287	-2.41	C <sub>9</sub> H <sub>16</sub> O <sub>5</sub> N	Pantothenic acid	L	97	7.45*	463.08820	463.08835	0.33	C <sub>21</sub> H <sub>20</sub> O <sub>12</sub>	Isoquercitrin	L
							S								
27	2.07	197.04555	197.04475	-4.04	C <sub>9</sub> H <sub>10</sub> O <sub>5</sub>	Danshensu	L	98	7.50*	593.15119	593.15063	-0.95	C <sub>27</sub> H <sub>30</sub> O <sub>15</sub>	Kaempferol-3-O-neohesperidoside	L
							S								

(continued on next page)

Table 1 (continued)

Peak	t <sub>R</sub>	Theoretical Mass m/z	Experimental Mass m/z	Error (ppm)	Formula	Identification/ Reactions	source	Peak	t <sub>R</sub>	Theoretical Mass m/z	Experimental Mass m/z	Error (ppm)	Formula	Identification/Reactions	source
28	2.07	315.07216	315.07220	0.14	C <sub>13</sub> H <sub>16</sub> O <sub>9</sub>	Protocatechuic acid-O-glucoside	L S	99	7.55	181.04954	181.04906	-2.62	C <sub>9</sub> H <sub>8</sub> O <sub>4</sub>	Caffeic acid isomer	L
29	2.15	167.03498	167.03498	-5.88	C <sub>8</sub> H <sub>8</sub> O <sub>4</sub>	Vanillic acid	L S	100	7.56	477.14023	477.13968	-1.16	C <sub>23</sub> H <sub>26</sub> O <sub>11</sub>	Calceolarioside B	L S
30	2.36	315.10854	315.10849	-0.16	C <sub>14</sub> H <sub>20</sub> O <sub>8</sub>	Hydroxytyrosol Glucoside	L S	101	7.59*	515.11950	515.11523	-8.29	C <sub>25</sub> H <sub>24</sub> O <sub>12</sub>	Isochlorogenic acid B	L
31	2.46	151.04006	151.03896	-7.33	C <sub>8</sub> H <sub>8</sub> O <sub>3</sub>	Isovanillin	L S	102	7.70*	447.09328	447.09396	1.51	C <sub>21</sub> H <sub>20</sub> O <sub>11</sub>	Luteolin 7-O-D-glucoside	L S
32	2.46	153.05572	153.05455	-7.63	C <sub>8</sub> H <sub>10</sub> O <sub>3</sub>	Hydroxytyrosol	L S	103	7.77	623.19814	623.19904	1.44	C <sub>29</sub> H <sub>36</sub> O <sub>15</sub>	Isoverbascoside	L S
33	2.55*	153.01933	153.01840	-6.09	C <sub>7</sub> H <sub>6</sub> O <sub>4</sub>	Protocatechuic acid	L S	104	8.03	623.16176	623.15649	-8.45	C <sub>28</sub> H <sub>32</sub> O <sub>16</sub>	Isorhamnetin-3-O-nehesperidine	L
34	2.60	167.03498	167.03401	-5.82	C <sub>8</sub> H <sub>8</sub> O <sub>4</sub>	Isovanillic acid	L S	105	8.10*	447.09328	447.09323	-0.12	C <sub>21</sub> H <sub>20</sub> O <sub>11</sub>	Kaempferol-7-O-glucoside	L S
35	3.08	151.04006	151.03894	-7.46	C <sub>8</sub> H <sub>8</sub> O <sub>3</sub>	(R)-Mandelic acid	L S	106	8.12	433.07763	433.07745	-0.43	C <sub>20</sub> H <sub>18</sub> O <sub>11</sub>	Quercetin pentoside	L S
36	3.20	389.10893	389.10889	-0.11	C <sub>16</sub> H <sub>22</sub> O <sub>11</sub>	Deacetylasperulosidic acid	L S	107	8.14*	187.09758	187.09671	-4.66	C <sub>9</sub> H <sub>16</sub> O <sub>4</sub>	Azelaic acid	L S
37	3.23	285.06159	285.06146	-0.46	C <sub>12</sub> H <sub>14</sub> O <sub>8</sub>	Dihydroxybenzoic acid pentoside isomer	L S	108	8.28	579.20831	579.20782	-0.85	C <sub>28</sub> H <sub>36</sub> O <sub>13</sub>	Syringaresinol-4'-O-glucopyranoside	L S
38	3.26	205.09715	205.09680	-1.73	C <sub>11</sub> H <sub>12</sub> N <sub>2</sub> O <sub>2</sub>	L-Tryptophan	L S	109	8.35*	193.05063	193.04976	-4.52	C <sub>10</sub> H <sub>10</sub> O <sub>4</sub>	Isoferulic acid	L S
39	3.30	375.12967	375.12949	-0.48	C <sub>16</sub> H <sub>24</sub> O <sub>10</sub>	Loganic acid	L	110	8.38	579.17083	579.17004	-1.37	C <sub>27</sub> H <sub>30</sub> O <sub>14</sub>	Rhoifolin	L
40	3.34	299.11363	299.11343	-0.66	C <sub>14</sub> H <sub>20</sub> O <sub>7</sub>	Salidroside	L S	111	8.44	447.09328	447.09241	-1.96	C <sub>21</sub> H <sub>20</sub> O <sub>11</sub>	Kaempferol-7-O-glucoside	L S
41	3.41	137.02442	137.02328	-8.30	C <sub>7</sub> H <sub>6</sub> O <sub>3</sub>	4-Hydroxybenzoic acid	L S	112	8.48	623.16176	623.15948	-3.65	C <sub>28</sub> H <sub>32</sub> O <sub>16</sub>	Narcissoside	L
42	3.49	175.06119	175.06021	-5.64	C <sub>7</sub> H <sub>12</sub> O <sub>5</sub>	2-isopropylmalic acid	L S	113	8.50	181.04954	181.04910	-2.40	C <sub>9</sub> H <sub>8</sub> O <sub>4</sub>	Caffeic acid isomer	L
43	3.56	153.01933	153.01820	-7.40	C <sub>7</sub> H <sub>6</sub> O <sub>4</sub>	Gentisic acid	L	114	8.57	301.07176	301.07181	0.16	C <sub>16</sub> H <sub>14</sub> O <sub>6</sub>	Hesperetin isomer	L
44	3.60	299.07724	299.07706	-0.60	C <sub>13</sub> H <sub>16</sub> O <sub>8</sub>	Salicylic acid-hexoside	L S	115	8.62	593.18758	593.18884	2.13	C <sub>28</sub> H <sub>34</sub> O <sub>14</sub>	Poncirin	L S
45	3.63	451.12458	451.12430	-0.63	C <sub>21</sub> H <sub>24</sub> O <sub>11</sub>	Catechin-glucopyranoside	L S	116	8.85	447.09328	447.09286	-0.95	C <sub>21</sub> H <sub>20</sub> O <sub>11</sub>	Quercetol-7-O-rhamnoside	L S
46	3.70	461.16645	461.16632	-0.28	C <sub>20</sub> H <sub>30</sub> O <sub>12</sub>	Forsythiaside E	L	117	9.07	607.16684	607.16681	-0.05	C <sub>28</sub> H <sub>32</sub> O <sub>15</sub>	Neodiosmin	L S
47	3.75	175.02481	175.02374	-6.12	C <sub>6</sub> H <sub>8</sub> O <sub>6</sub>	Ascorbic acid isomer	L	118	9.46	447.09328	447.09314	-0.32	C <sub>21</sub> H <sub>20</sub> O <sub>11</sub>	Quercetol-7-O-rhamnoside	L S
48	3.93	341.08780	341.08746	-1.01	C <sub>15</sub> H <sub>18</sub> O <sub>9</sub>	CA-hexoside	L S	119	9.76	447.09328	447.09299	-0.66	C <sub>21</sub> H <sub>20</sub> O <sub>11</sub>	Quercetin-3-rhamnoside	L S
49	3.95	181.04954	181.04915	-2.13	C <sub>9</sub> H <sub>8</sub> O <sub>4</sub>	Caffeic acid isomer	L	120	10.06*	263.12888	263.12863	-0.96	C <sub>15</sub> H <sub>20</sub> O <sub>4</sub>	Abcsicic acid	L S
50	3.98	431.15588	431.15549	-0.92	C <sub>19</sub> H <sub>28</sub> O <sub>11</sub>	Osmanthuside H	L S	121	10.23*	287.05611	287.05594	-0.60	C <sub>15</sub> H <sub>12</sub> O <sub>6</sub>	Eriodictyol	L S
51	4.05	131.07136	131.07014	-9.36	C <sub>6</sub> H <sub>12</sub> O <sub>3</sub>	2-hydroxyhexanoic acid or isomer	L	122	10.82	201.11323	201.11243	-3.99	C <sub>10</sub> H <sub>18</sub> O <sub>4</sub>	3-tert-Butylpropionic acid	L S
52	4.19	323.13475	323.13446	-0.91	C <sub>13</sub> H <sub>24</sub> O <sub>9</sub>	Periplobiose	L S	123	12.19	283.06119	283.06094	-0.9	C <sub>16</sub> H <sub>12</sub> O <sub>5</sub>	Calycosin	L
53	4.24	167.03498	167.03392	-6.36	C <sub>8</sub> H <sub>8</sub> O <sub>4</sub>	Orsellinic acid	L S	124	12.22	301.03537	301.03516	-0.72	C <sub>15</sub> H <sub>10</sub> O <sub>7</sub>	Quercetin isomer	L
54	4.26	163.04007	163.03886	-7.40	C <sub>9</sub> H <sub>8</sub> O <sub>3</sub>	2-Coumaric acid	L S	125	12.26*	285.04046	285.04025	-0.74	C <sub>15</sub> H <sub>10</sub> O <sub>6</sub>	Luteolin	L
55	4.31	151.04006	151.03893	-7.53	C <sub>8</sub> H <sub>8</sub> O <sub>3</sub>	vanillin	L S	126	12.86	301.07176	301.07138	-1.27	C <sub>16</sub> H <sub>14</sub> O <sub>6</sub>	Hesperetin	L

(continued on next page)

Table 1 (continued)

Peak	t <sub>R</sub>	Theoretical Mass m/z	Experimental Mass m/z	Error (ppm)	Formula	Identification/Reactions	source	Peak	t <sub>R</sub>	Theoretical Mass m/z	Experimental Mass m/z	Error (ppm)	Formula	Identification/Reactions	source
56	4.31*	289.07176	289.07147	-1.02	C <sub>15</sub> H <sub>14</sub> O <sub>6</sub>	Catechin	L S	127	12.92	373.12818	373.12759	-4.52	C <sub>20</sub> H <sub>20</sub> O <sub>7</sub>	sinensetin	L
57	4.35	181.04954	181.04921	-1.80	C <sub>9</sub> H <sub>8</sub> O <sub>4</sub>	Caffeic acid isomer	L	128	13.22	269.04555	269.04559	0.16	C <sub>15</sub> H <sub>10</sub> O <sub>5</sub>	Genistein	L S
58	4.38	285.06159	285.06137	-0.77	C <sub>12</sub> H <sub>14</sub> O <sub>8</sub>	Dihydroxyben-zoic acid pentoside	L S	129	13.24	299.09250	299.09213	-1.23	C <sub>17</sub> H <sub>16</sub> O <sub>5</sub>	Farrerol	L
59	4.40	341.08780	341.08740	-1.19	C <sub>15</sub> H <sub>18</sub> O <sub>9</sub>	CA-hexoside	L S	130	13.31*	285.04046	285.04025	-0.74	C <sub>15</sub> H <sub>10</sub> O <sub>6</sub>	Kaempferol	L S
60	4.66*	353.08781	353.08765	-0.44	C <sub>16</sub> H <sub>18</sub> O <sub>9</sub>	Cryptochlorogenic acid	L	131	13.38	299.05611	299.05600	-0.37	C <sub>16</sub> H <sub>12</sub> O <sub>6</sub>	Chrysoeriol	L S
61	4.75	131.07136	131.07018	-9.06	C <sub>6</sub> H <sub>12</sub> O <sub>3</sub>	2-hydroxyhexanoic acid or isomer	L	132	13.43*	315.05103	315.05099	-0.11	C <sub>16</sub> H <sub>12</sub> O <sub>7</sub>	Isorhamnetin	L
62	4.75*	353.08781	353.08670	-3.13	C <sub>16</sub> H <sub>18</sub> O <sub>9</sub>	Chlorogenic acid	L	133	13.92	299.05611	299.05582	-0.97	C <sub>16</sub> H <sub>12</sub> O <sub>6</sub>	Chrysoeriol isomer	L S
63	4.78	289.07176	289.07083	-3.22	C <sub>15</sub> H <sub>14</sub> O <sub>6</sub>	Epicatechin	L S	134	14.37	283.06119	283.06094	-0.91	C <sub>16</sub> H <sub>12</sub> O <sub>5</sub>	Genkwanin	L S
64	4.92*	179.03498	179.03395	-5.76	C <sub>9</sub> H <sub>8</sub> O <sub>4</sub>	Caffeic acid	L S	135	14.41	373.12818	373.12723	-2.54	C <sub>20</sub> H <sub>20</sub> O <sub>7</sub>	Isosinensetin	L S
65	4.94	517.15628	517.15601	-0.52	C <sub>22</sub> H <sub>30</sub> O <sub>14</sub>	Ferulic acid dihexoside	L S	136	14.53	311.22278	311.22275	-0.10	C <sub>18</sub> H <sub>32</sub> O <sub>4</sub>	Dihydroxyoctadecadienoic acid	L S
66	4.99	355.10345	355.10324	-0.61	C <sub>16</sub> H <sub>20</sub> O <sub>9</sub>	Ferulic Acid-hexoside	L S	137	14.90	389.12309	389.12195	-2.94	C <sub>20</sub> H <sub>20</sub> O <sub>8</sub>	Demethylnobiletin	L S
67	5.30	625.14102	625.14136	0.54	C <sub>27</sub> H <sub>30</sub> O <sub>17</sub>	Quercetin dihexoside	L S	138	14.91	487.34289	487.34259	-0.63	C <sub>30</sub> H <sub>48</sub> O <sub>5</sub>	Tormentic acid	L S
68	5.55	355.10345	355.10327	-0.52	C <sub>16</sub> H <sub>20</sub> O <sub>9</sub>	Ferulic Acid-hexoside	L S	139	15.03	311.22278	311.22281	0.09	C <sub>18</sub> H <sub>32</sub> O <sub>4</sub>	Dihydroxyoctadecadienoic acid isomer	L S
69	5.69	163.04007	163.03908	-6.06	C <sub>9</sub> H <sub>8</sub> O <sub>3</sub>	3-Coumaric acid	L S	140	15.77	389.12309	389.12213	-2.48	C <sub>20</sub> H <sub>20</sub> O <sub>8</sub>	Demethylnobiletin isomer	L S
70	5.82	449.10893	449.10855	-0.86	C <sub>21</sub> H <sub>22</sub> O <sub>11</sub>	Taxifolin 7-rhamnoside	L	141	16.45	277.21730	277.21695 279.23120	-1.27	C <sub>18</sub> H <sub>30</sub> O <sub>2</sub>	α-Linolenic acid isomer	L S
71	5.87	593.15119	593.15088	-0.53	C <sub>27</sub> H <sub>30</sub> O <sub>15</sub>	Vicenin II	L S	142	19.33	277.21730	277.21692	0.59	C <sub>18</sub> H <sub>30</sub> O <sub>2</sub>	α-Linolenic acid	L S

\* identified by comparison with reference standards.

L: leaf, S: stem.

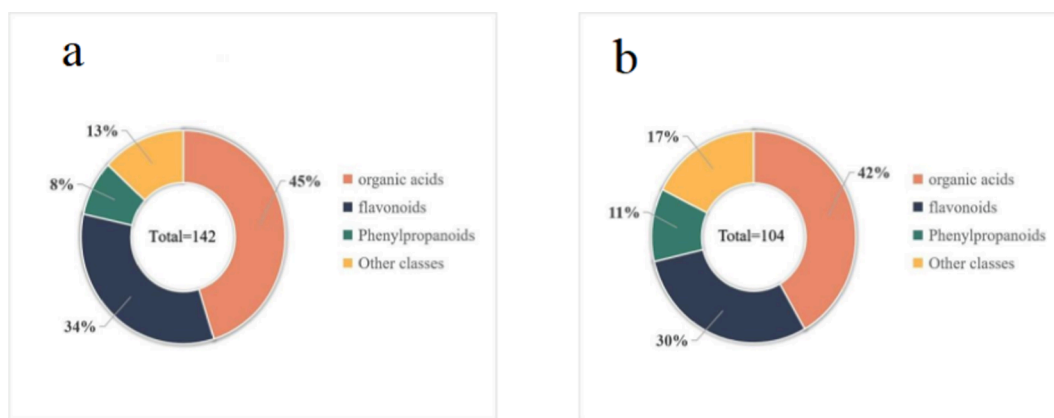


Fig. 1. A total of 142 and 104 compounds were identified in the leaf (a) and stem (b) of *A. macrotera*.

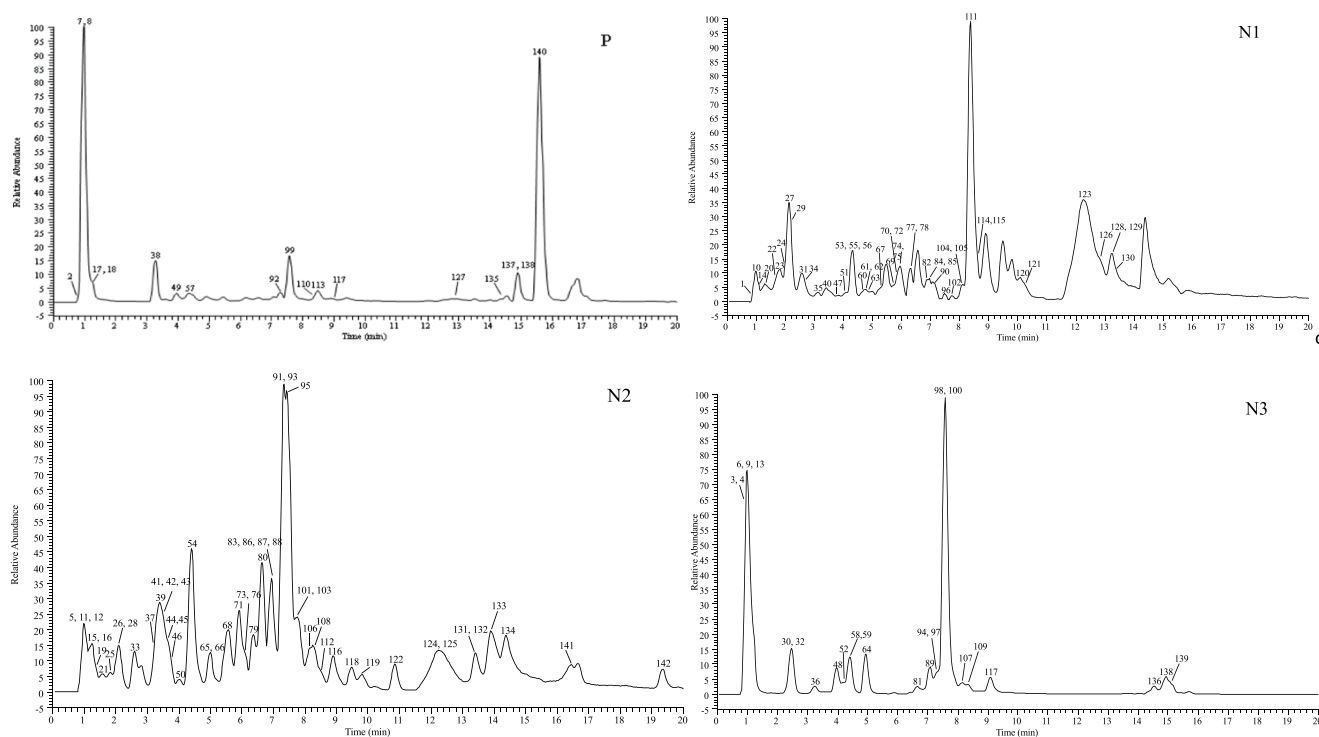


Fig. 2. The high-resolution extracted ion chromatograms (EICs) of *A. macrotera*. (P) for positive and (N1-N3) for negative ion mode.

### 3.2.2. Identification of organic acids

Peaks 1, 9, 10, 13, 15, 16, 21, 33, 60, 62, 64, 76, 78, 85, 93, 101, 107, 109, and 120 were accurately identified as quinic acid, malic acid,  $\alpha$ -ketoglutaric acid, citric acid, citraconic acid, *cis*-aconitic acid, gallic acid, protocatechuic acid, cryptochlorogenic acid, chlorogenic acid, caffeic acid, 4-coumaric acid, suberic acid, ferulic acid, salicylic acid, isochlorogenic acid B, azelaic acid, isoferulic acid, and abscisic acid. This identification was based on the retention time and MS<sup>2</sup> pattern of the corresponding reference standard.

Peak 44 contained a [M-H]<sup>-</sup> ion at  $m/z$  299.0772, and a fragment ion at  $m/z$  137.0231 [M-H-C<sub>6</sub>H<sub>10</sub>O<sub>5</sub>]<sup>-</sup>, corresponding to the loss of a hexose, and then by the neutral loss of a CO<sub>2</sub>, a fragment ion of  $m/z$  93.0332 [M-H-C<sub>6</sub>H<sub>10</sub>O<sub>5</sub>-CO<sub>2</sub>]<sup>-</sup> was identified. Thus, peak 44 was considered to be salicylic acid-hexoside. By comparing with databases and retention time behavior, peaks 48 and 59 showed similar [M-H]<sup>-</sup> ions at  $m/z$  341.08780 and produced fragment ions at  $m/z$  179.0339 [M-H-C<sub>6</sub>H<sub>10</sub>O<sub>5</sub>]<sup>-</sup> and 135.0438 [M-H-C<sub>6</sub>H<sub>10</sub>O<sub>5</sub>-CO<sub>2</sub>]<sup>-</sup>, respectively. Thus, they were characterized as caffeic acid-hexoside (Tang et al.,

2022). Peaks 66, 68 and 73 possessed the deprotonation ion [M-H]<sup>-</sup> at  $m/z$  355.1035, and displayed fragment ions at  $m/z$  193.0497 [M-H-C<sub>6</sub>H<sub>10</sub>O<sub>5</sub>]<sup>-</sup>, 175.0390 [M-H-C<sub>6</sub>H<sub>10</sub>O<sub>5</sub>-H<sub>2</sub>O]<sup>-</sup>, and 149.0596 [M-H-C<sub>6</sub>H<sub>10</sub>O<sub>5</sub>-CO<sub>2</sub>]<sup>-</sup>. By comparison with the literature, these peaks were assigned as ferulic acid-hexoside (Mena et al., 2018).

Peaks 11, 24, 27, 35, 41, 42, 43, 54, and 69 were respectively characterized as *trans*-aconitic acid, geniposidic acid, danshensu, (r)-mandelic acid, 4-hydroxybenzoic acid, 2-isopropylmalic acid, gentisic acid, 2-coumaric acid and 3-coumaric acid by comparison with mzVault.

Peak 12 exhibited a [M-H]<sup>-</sup> ion at  $m/z$  175.0248, which was characterized as ascorbic acid, and yielded fragment ions at  $m/z$  146.9599 and 130.8732, in accordance with the previously reported data (Luo et al., 2020). According to the MS<sup>2</sup> data and retention time behavior reported in the literature (Li et al., 2020), peaks 14, 19 were identified as tartaric acid, mevalonic acid. Peaks 29, 34, 53, and 72 were characterized as vanillic acid, orsellinic acid, isovanillic acid and 4-methoxysalicylic acid (Wang et al., 2021). Peak 26, with a [M-H]<sup>-</sup> ion at  $m/z$  218.1034, produced a fragment ion at  $m/z$  146.0810, which was

identified as pantothenic acid when comparing with previously reported data (Shi et al., 2022). Coincidentally, the peaks 51 and 61 displayed a molecular ion with a mass of 131.0714  $[M-H]^-$  and generated a product ion at  $m/z$  87.0437  $[M-H-CO_2]^-$  and 85.0644  $[M-H-CO_2-2H]^-$ , which corresponds to a loss of  $CO_2$ . Thus, they were proposed to be 2-hydroxyhexanoic acid or its isomer according to published data (Li et al., 2020). Peaks 31 and 55 showed a similar  $[M-H]^-$  ion at  $m/z$  151.0401 and produced a fragment ion at  $m/z$  108.0441  $[M-H-CO_2]^-$ . By comparing with databases and considering their retention time behavior, they were respectively characterized as isovanillin and vanillin (Koprivica et al., 2018). Peak 65 gave a  $[M-H]^-$  ion at  $m/z$  517.1563 and a major fragment ion at  $m/z$  193.0497 and was identified as ferulic acid-dihexoside, in agreement with the literature (Koprivica et al., 2018). Peaks 37 and 58 gave the same  $[M-H]^-$  ion at  $m/z$  285.0616, as well as ions at  $m/z$  152.0103, 153.0183, 108.0202 and 109.0282, and were thus identified as dihydroxybenzoic acid pentoside or its isomer, in accordance with the literature (Peixoto Araujo et al., 2020). Peak 122, with a  $[M-H]^-$  ion at  $m/z$  201.1132, produced fragment ions at  $m/z$  139.1116 and 183.1016, which was identified as 3-*tert*-butylpropionic acid by comparing with public data (Yu et al., 2019).

In the characterization, a total of 65 types of organic acids and their derivatives were identified in the leaf, whereas only 45 types of compounds were detected in the stem. For example, substances such as gallic acid, geniposidic acid, gentisic acid, and chlorogenic acid, were only found in leaf. Thus, the antioxidant activity of the leaf may be more effective than the stem.

### 3.2.3. Identification of phenylpropanoids and their derivatives

The majority of phenylethanol glycosides (phgs) have a class of phgs with a caffeoyl group, therefore, the  $MS^2$  of most compounds will show the same fragment pattern attributed to the caffeoyl group at  $m/z$  161.0232, 135.0438 and 179.0340 (Han et al., 2012), which can therefore be used as diagnosis ions of phenylethanol glycosides. Peak 100 showed the  $[M-H]^-$  ion at  $m/z$  477.1402 and produced a fragment ion at  $m/z$  315.1084  $[M-H-C_6H_6O_3]^-$  and 161.0234  $[M-H-C_8H_{10}O_3-C_6H_{10}O_5]^-$ , which indicated the presence of phenethyl glycosides. Thus, it was speculated as calceolarioside B. Analogously, peaks 89 and 95, displayed secondary fragment ions with roughly the same  $m/z$  of 161.0232, 179.0340 and 135.0438, which are typical of phenylethanol glycosides. Therefore, peaks 89 and 95 were identified as verbascoside, and isoverbascoside, respectively. (Huang et al., 2010).

Peak 32 was detected at  $m/z$  153.0557, with a fragment ion at  $m/z$  123.0438, corresponding to the loss of a  $CH_2OH$  group, and was thus identified as hydroxytyrosol (Peralbo-Molina et al., 2012). Peak 30 carried the precursor  $[M-H]^-$  ion at  $m/z$  315.1085 and yielded the main ions at  $m/z$  153.0545  $[M-H-C_6H_{10}O_5]^-$ , 123.0437 and 135.0438, which suggested the presence of hydroxytyrosol. Therefore peak 30 was characterized as hydroxytyrosol-glucoside (Peralbo-Molina et al., 2012).

Peak 40 exhibited the  $[M-H]^-$  at  $m/z$  299.1136, which gave its product ion at  $m/z$  137.0233 and 119.0487, affirmed as salidroside according to published data (Li et al., 2017). Peak 46 was characterized as forsythiaside E by comparison with the databases. Peak 50 was detected at  $m/z$  431.1559, with the main characteristic ion at  $m/z$  229.1136, corresponding to the neutral loss of the furanosyl group in the precursor  $[M-H]^-$  ion, which is consistent with the fragmentation of osmanthoside H (Huang et al., 2010).

Peaks 89, 95, and 103 were identified as  $\beta$ -hydroxyverbascoside, verbascoside and isoverbascoside, respectively. Peaks 75 and 77 possessed an identical precursor ion at  $m/z$  415.1610  $[M-H]^-$  and produced the same fragment ions at  $m/z$  161.0442 and 101.0230. Thus, these peaks were identified as phenylethylrutinoside by comparing with public data (Zeng et al., 2017). Peak 108 showed a deprotonated ion  $[M-H]^-$  at  $m/z$  579.2083 and produced a major fragment ion at  $m/z$  417.1549  $[M-H-C_6H_{10}O_5]^-$  corresponding to the loss of a glucose, hence it was identified as syringaresinol 4-*O*- $\beta$ -D-glucopyranoside on the basis of literature (Liu et al., 2022).

A total of 12 substances were found and characterized as phenylpropanoid and its derivatives, of which forsythiaside E was only detected in the leaf. Forsythiaside E may be the main characteristic component of the leaf.

### 3.2.4. Identification of other classes of compounds

A total of 19 other classes of compounds were detected in the leaf and stem extracts of the *A. macrotera*. This includes amino acids, sugars, alkaloids, and unsaturated fatty acids. For example, by comparing peak 18 with a reference public data set, peak 18 was determined to be l-tyrosine, (Jin et al., 2022) and amino acid of interest. It produced a precursor ion at  $m/z$  182.0812  $[M+H]^+$  and diagnostic ions at  $m/z$  136.0756  $[M+H-CO_2]^+$  and 119.0491  $[M+H-CO_2-OH]^+$  in the positive-ion mode. Analogously, peaks 2, 7, 25, and 38 were assigned to arginine, l-glutamic acid, l-phenylalanine, and l-tryptophan, respectively.

## 3.3. Antioxidant analysis of the *A. macrotera*

### 3.3.1. DPPH free radical scavenging assay

The antioxidant activity of the leaf and stem extract were first determined by measuring the DPPH scavenging capacity, which showed that these extracts had a good scavenging activity against DPPH radicals. As shown in Fig. 3(a), the extracts of leaf and stem, at concentrations of 0.0025–0.15 mg/mL, showed dose-dependent effects of DPPH radical clearance with an the biochemical half maximal inhibitory concentration ( $IC_{50}$ ) value of 0.019 and 0.067 mg/mL, respectively. Notably, the leaf extract at 0.1 mg/mL concentration showed a  $91.53 \pm 1.85$  % clearance of DPPH radicals, with a better clearance of DPPH radicals than the stem extract.

### 3.3.2. ABTS free radical scavenging assay

The clearance ability of ABTS radicals by the leaf and stem extract is shown in Fig. 3(b). The results showed that the extracts of leaf and stem, at concentrations of 0.005–0.15 mg/mL, showed dose-dependent effects of ABTS radical clearance with an  $IC_{50}$  value of 0.03 and 0.05 mg/mL, respectively. In particular, the leaf extract at 0.1 mg/mL concentration showed a  $95.4 \pm 2.15$  % clearance of ABTS radicals, with a better ABTS radical clearance than the stem extract.

### 3.3.3. Hydroxyl free radical scavenging assay

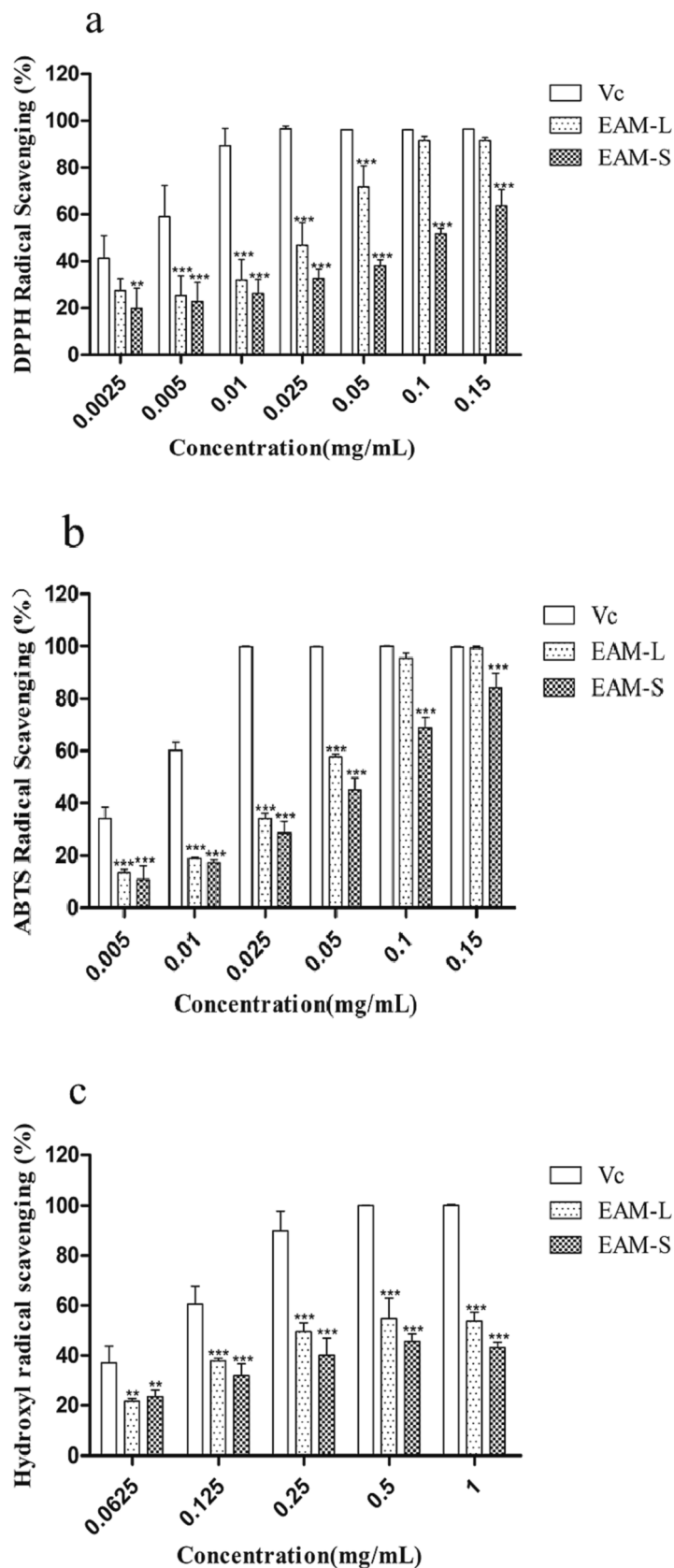
As shown in Fig. 3(c), the leaf and stem extract at a concentration of 0.5 mg/mL showed a  $54.84 \pm 8.25$  % and  $45.64 \pm 3.04$  % clearance, respectively, to the hydroxyl radicals, with an  $IC_{50}$  value of 0.347 and 0.558 mg/mL, respectively. The experimental results indicate that both the leaf and stem extract had a good scavenging effect on the hydroxyl free radicals.

### 3.3.4. FRAP and CUPRAC/antioxidant capacity assays for the reduction of transition metal ions

The FRAP assay and the CUPRAC assay were conducted to measure the antioxidant potential of the plant extracts to reduce iron and copper ions. As shown in Fig. 4, the FRAP determines the ability to reduce  $Fe^{3+}$  to  $Fe^{2+}$ , while CUPRAC determines the ability to reduce  $Cu^{2+}$  to  $Cu^+$ . *A. macrotera* extracts were found to be more effective in reducing iron and copper ions with increasing concentrations. Extraction of *A. macrotera* exhibited a good ability to reduce transition metal ions. For example, at the concentration of 1 mg/mL, the iron ion reduction capacity of the leaf and stem extract was found to be  $1.785 \pm 0.089$  and  $0.67 \pm 0.022$  mmol/L, respectively. A high level of active compounds, such as polyphenolic compounds, may make the extracts capable of reducing transition metal ions.

### 3.3.5. Relationship between the identified compounds and antioxidant

The above antioxidant experiments indicate that the overall antioxidant activity of the leaf extract is better than that of the stem extract.



(caption on next page)

**Fig. 3.** Effect of DPPH radical scavenging of the *A. macrotera* extracts. Among them, VC represents vitamin C, EAM-L represents leaf extract, and EAM-S represents stem extract. Different concentrations of the extracts and Vc (final concentrations of 0.0025, 0.005, 0.01, 0.025, 0.05, 0.1 and 0.15 mg/mL). a. Effect of ABTS radical scavenging of the *A. Macrotera* extracts. Different concentrations of the extract and Vc (final concentrations of 0.005, 0.01, 0.025, 0.05, 0.1 and 0.15 mg/mL, respectively). b. Hydroxyl radical scavenging action of the *A. Macrotera* extracts. Different concentrations of the extracts and Vc (final concentrations of 0.0625, 0.125, 0.25, 0.5 and 1.0 mg/mL, respectively). c. Data are presented as the means  $\pm$  SD of three independent experiments, \* is compared to the Vc group, \*P < 0.05, \*\*P < 0.01, \*\*\*P < 0.005.

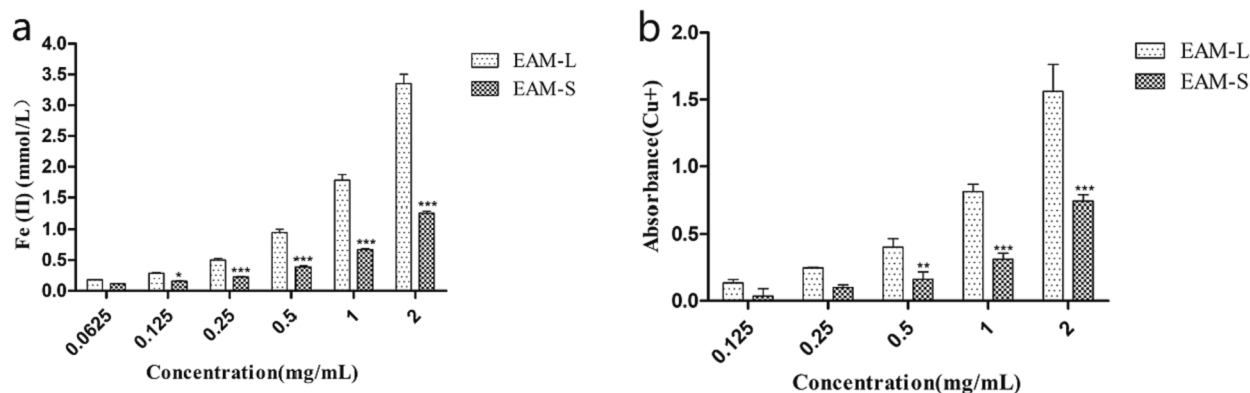


**Fig. 4.** The ability of the *A. macrotera* extracts to reduce ferric ions ( $\text{Fe}^{3+}$ ) to ferrous ions ( $\text{Fe}^{2+}$ ). EAM-L represents leaf extract, and EAM-S represents stem extract. Different concentrations of the extracts. (final concentrations of 0.0625, 0.125, 0.25, 0.5, 1 and 2 mg/mL). b. The ability of the *A. macrotera* extracts to reduce Copper ions ( $\text{Cu}^{2+}$ ) to Cuprous ions ( $\text{Cu}^{+}$ ). EAM-L represents leaf extract, and EAM-S represents stem extract. Different concentrations of the extracts. (final concentrations of 0.0625, 0.125, 0.25, 0.5, 1 and 2 mg/mL). \* is compared to the EAM-L. \*P < 0.05, \*\*P < 0.01, \*\*\*P < 0.005.

This finding aligns with our prior component characterization of the extracts. Specifically, during the component identification experiment, a total of 65 organic acids were identified in the leaf extract, whereas only 45 were detected in the stem extract. Furthermore, substances such as gallic acid were only detected in the leaf extract, indicating that organic acid compounds have excellent antioxidant capabilities. Compounds such as gallic acid have been empirically demonstrated to possess commendable antioxidant properties (Badhani et al., 2015), which corroborates why the leaf appears to have better antioxidant capacity compared to the stem.

#### 3.4. Anti-tyrosinase activities of different extracts

In this experiment, the *A. macrotera* extracts showed a relatively better inhibition with an  $\text{IC}_{50}$  value of 2.479 mg/mL (leaf extract) and

23.03 mg/mL (stem extract), respectively. In this study, the leaf extract was shown to have a better ability to inhibit tyrosinase than the stem extract (Fig. 5).

This is consistent with our previous natural activity identification experiments. The  $\text{IC}_{50}$  value of the leaf extract is lower than the stem extract, which may be closely related to the higher abundance of flavonoids, organic acids, and phenylpropanoids in the leaf. In natural-medicinal plants, the interaction between various components may produce unexpected results, and flavonoids and organic acid compounds are rich in anti-tyrosinase activities, which has been confirmed in the literature (Chen et al., 2022). In traditional Chinese medicine, phenylpropanoid compounds have demonstrated commendable efficacy in inhibiting tyrosinase activity (Li et al., 2023). It is worth noting that among the 12 phenylpropanoid compounds identified, forsythiaside E solely manifested in the leaf extract. Such findings imply the potential of

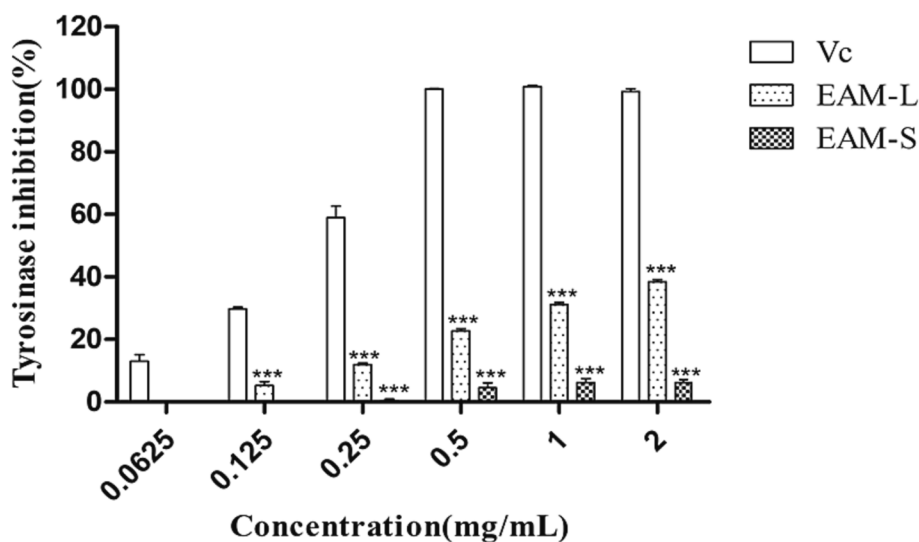


**Fig. 5.** Inhibition of tyrosinase activity by the *A. macrotera*. Among them, VC represents vitamin C, EAM-L represents leaf extract, and EAM-S represents stem extract. Different concentrations of the extracts and Vc (final concentrations of 0.0625, 0.125, 0.5, 1, and 2 mg/mL). \* is compared to the Vc. \*\*\*P < 0.005.

forsythiaside E as a potent anti-tyrosinase agent, thereby corroborating prior research outcomes (Niu et al., 2020).

### 3.5. Cell experiments of the *A. macrotera* extracts

#### 3.5.1. Effects of the *A. macrotera* extracts on the viability of RAW264.7 cells

To test the potential cytotoxicity of the leaf and stem extract against RAW264.7 cells, the cell viability was determined by the MTT assay. A variety of concentrations of leaf and stem extract (0.1, 0.2, and 0.4 mg/mL) were applied to cells for 24 h. As shown in Fig. 6(a), none of the cells treated with these extracts showed any cytotoxicity.

#### 3.5.2. NO assay

To investigate the anti-inflammatory potential of the leaf and stem extract, we determined the levels of NO (a key proinflammatory cell mediator) in the supernatant of the cells treated with LPS using the Griess reagent. NO production was inhibited in the LPS-treated cells by pretreatment with leaf and stem extract in RAW264.7 cells, as shown in Fig. 6(b). As a result, pretreatment of the cells showed significant and dose-dependent inhibition with leaf and stem extract. Therefore, our results indicate that leaf and stem extract can inhibit the generation of inflammatory mediators of macrophages treated with LPS. This may be a source of a novel anti-inflammatory agent.

#### 3.5.3. Relationship between the identified compounds and anti-inflammatory

The above cell experiments indicate that the overall anti-inflammatory activity of leaf extract is better than that of stem extract. This finding aligns with our prior component characterization of the two extracts. Specifically, during the component identification experiment, a total of 48 flavonoids were identified in the leaf extract, whereas only 32 were detected in the stem extract. Furthermore, in the quantitative experiments, the leaf extract consisted of 22 % of flavonoids while the stem extract contained only 9 %. The significant anti-inflammatory capacity of flavonoids has previously been confirmed in the literature (Maleki et al., 2019).

## 4. Conclusions

In this study, the phytochemical characterization of the antioxidant and anti-inflammatory properties of *A. macrotera* are examined. For the first time, UHPLC-Q-Exactive Orbitrap MS was used to efficiently characterize 142 chemicals, including flavonoids, phenolic acids, and phenylpropanoids. Amongst them, all 142 compounds were found in the leaf while 104 were found in the stem. The results of content determination revealed that *A. macrotera* leaves are made up of polysaccharides (55 %), polyphenols (35 %) and flavonoids (22 %), while the stems are made up of polysaccharides (35 %), polyphenols (20 %) and flavonoids (9 %). The activity results showed that the leaf extract and stem extract had strong scavenging effects on both DPPH, ABTS and  $\bullet$ OH radicals, and also had a significant reduction capacity for the reduction of both iron and copper metal ions. The antioxidant capacity of the leaf extract was found to be much better than that of the stem extract, which may be due to the high content of polysaccharide, flavonoids, and polyphenol in the leaf. Tyrosinase inhibition experiments also showed that the leaf extract had a stronger inhibition effect on the tyrosinase activity than the stem extract, which may possibly be related to the abundant compounds found in the extracts. The extracts both showed a strong inhibition of NO production from RAW264.7 cells, with a dose-dependent inhibition.

This study has established phytochemical characterization, the antioxidant characteristics of the *A. macrotera* leaf and stem, and evaluation of cytotoxicity and NO release assays. This method will serve as a benchmark to establish quality standards, as well as for the development and utilization of *A. macrotera* in the future.

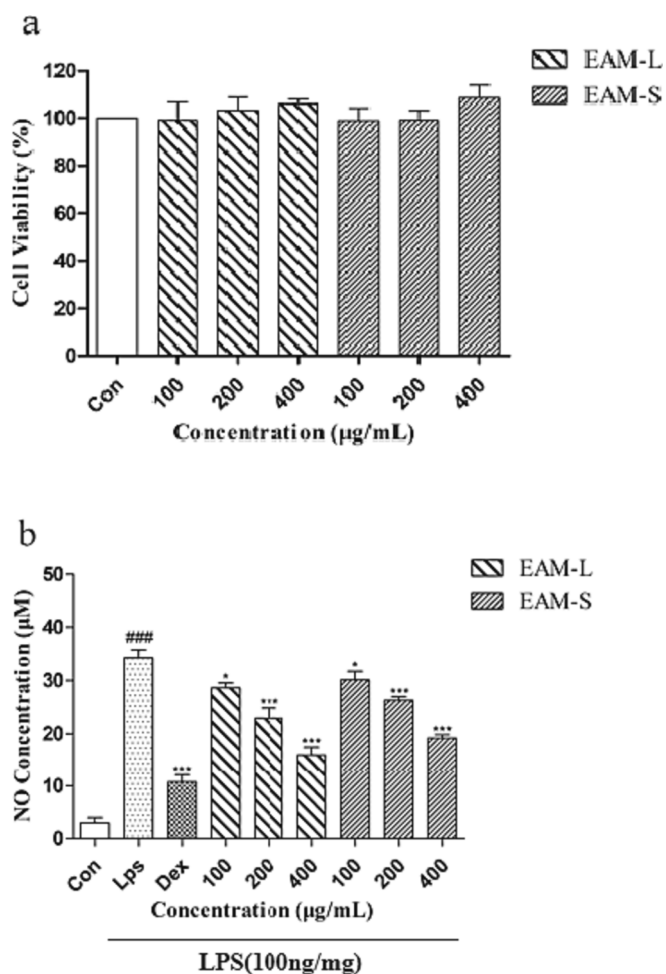


Fig. 6. Protective effects of EAM-L and EAM-S against the LPS-induced oxidative stress in RAW264.7 cells. EAM-L represents leaf extract, and EAM-S represents stem extract. a. RAW264.7 cells were treated with different concentrations (final concentrations of 100, 200 and 400 µg/mL) of EAM-L and EAM-S for 24 h, and the cell viability was determined by the MTT assay. b. RAW264.7 cells were pre-treated with different concentrations of EAM-L and EAM-S for 1 h before treatment with LPS(100 ng/mL), the concentration of dexamethasone is 1 µM and then were treated with 100 ng/mL of LPS for 18 h to detect the amount of no release. Data are presented as the mean  $\pm$  SD of three independent experiments, # is compared to the con group, \* is compared to the LPS group, ### $P < 0.05$ , \* $P < 0.05$ , \*\* $P < 0.01$ , \*\*\* $P < 0.005$ .

### CRediT authorship contribution statement

**Kaiquan Yu:** Writing – original draft, Writing – review & editing. **Jian Li:** Writing – original draft, Writing – review & editing. **Yuqi Chen:** . **Min Zhang:** . **Jiaxin Li:** Software. **Shani Li:** Software. **Qing Li:** . **Ling Liu:** . **Lilan Yi:** Methodology, Writing – review & editing, Supervision, Project administration. **Qingjiao He:** Methodology, Writing – review & editing, Supervision, Project administration, Funding acquisition.

### Declaration of competing interest

The authors declare that they have no known competing financial interests or personal relationships that could have appeared to influence the work reported in this paper.

### Acknowledgments

This research received no funding. This project was supported by Hunan Province Social Science Innovation Research Base (Ethnic

medicine and ethnic culture research base).

## Appendix A. Supplementary material

Supplementary data to this article can be found online at <https://doi.org/10.1016/j.arabjc.2023.105575>.

## References

- Aras, A., Bursal, E., Alan, Y., et al., 2018. Polyphenolic content, antioxidant potential and antimicrobial activity of *Satureja boissieri*. Iran. J. Chem. Chem. Eng. 37, 209–219.
- Badhani, B., Sharma, N., Kakkar, R., 2015. Gallic acid: A versatile antioxidant with promising therapeutic and industrial applications. RSC Adv. 5, 27540–27557.
- Bai, Y.L., Hong, Z.D., Zhang, T.Y., Cai, B.D., Zhang, Y.-Z., Feng, Y.Q., 2020. A method for simultaneous determination of 14 carbonyl-steroid hormones in human serum by ultra high performance liquid chromatography-tandem mass spectrometry. J. Anal. Test. 4 (1), 1–12.
- Chen, W.-C., Wang, S.-W., Li, C.-W., et al., 2022. Comparison of various solvent extracts and major bioactive components from *Portulaca oleracea* for antioxidant, anti-tyrosinase, and anti- $\alpha$ -glucosidase activities. Antioxidants. 11, 398.
- F.o.C.E. Committee, 2018. Flora of China. Flora of China.
- Delgado, A.M., Issaoui, M., Chammem, N., 2019. Analysis of main and healthy phenolic compounds in foods. J. AOAC Int. 102 (5), 1356–1364.
- Duan, X.C., Chang, F., Yang, X.G., Liu, Z.L., Yang, J., 2014. Nutritional components of *Abelia engleriana* tender leaves and characteristics and antioxidant activity of their polysaccharide gel extracts. Food Sci. 35 (13), 103–107.
- Han, L.F., Boakye-Yiadom, M., Liu, E.W., Zhang, Y., Li, W., Song, X.B., Fu, F., Gao, X.-M., 2012. Structural characterisation and identification of phenylethanoid glycosides from *Cistanche deserticola* Y.C. Ma by UHPLC/ESI-QTOF-MS/MS. Phytochem. Anal. 23 (6), 668–676.
- Hou, C., Chen, L., Yang, L., Ji, X., 2020. An insight into anti-inflammatory effects of natural polysaccharides. Int. J. Biol. Macromol. 153, 248–255.
- Huang, X.J., Yin, Z.Q., Ye, W.C., Shen, W.B., 2010. Chemical constituents from fruits of *Ligustrum lucidum*. China J. Chin. Mater. Med. 35 (07), 861–864.
- Jin, Y., Cheng, S., Liu, R., Yu, C., Zhang, L., Li, X.L., Yan, G., Zheng, M., Zhe Min, J., 2022. Comprehensive characterization of the chemical composition of *Lurong dabu* decoction and its absorbed prototypes and metabolites in rat plasma using UHPLC-Q Exactive Orbitrap-HRMS. Food Res. Int. 161, 111852.
- Klomsakul, P., Aiumsubtub, A., Chalopagorn, P., 2022. Evaluation of antioxidant activities and tyrosinase inhibitory effects of *Ginkgo biloba* tea extract. Sci. World J. 2022, 4806889.
- Koprivica, M.R., Trifković, J.D., Dramićanin, A.M., Gašić, U.M., Akšić, M.M.F., Milojković-Opšencica, D.M., 2018. Determination of the phenolic profile of peach (*Prunus persica* L.) kernels using UHPLC-LTQ Orbitrap MS/MS technique. Eur. Food Res. Technol. 244 (11), 2051–2064.
- Kuppusamy, P., Yusoff, M.M., Parine, N.R., Govindan, N., 2015. Evaluation of in-vitro antioxidant and antibacterial properties of *Commelina nudiflora* L. extracts prepared by different polar solvents. Saudi J. Biol. Sci. 22 (3), 293–301.
- Lee, J.S., Song, I.H., Shinde, P.B., Nimse, S.B., 2020. Macrocycles and supramolecules as antioxidants: Excellent scaffolds for development of potential therapeutic agents. Antioxidants 9 (9), 859.
- Li, K.L., Xiong, P., Gong, K.Y., Peng, J., Shi, S.L., Cai, W., 2020. Rapid characterization of constituents in *Duhalea nervosa* based on UHPLC-Q-Exactive Orbitrap MS combined with exclusion list technique. Nat. Prod. Res. Dev. 32 (02), 250–256.
- Li, H.L., Yang, L., Xiang, L.C., Cao, F.J., Liu, M., Wang, X.B., Feng, Y.B., 2015. Influence of different extracted methods on anti-oxidative activity of pectin extracting from *Abelia macrotera* leaves of Wudang Mountain Area. HUM J. 34 (06), 552–555.
- Li, H., Yao, W., Liu, Q., Xu, J., Bao, B., Shan, M., Cao, Y., Cheng, F., Ding, A., Zhang, L., 2017. Application of UHPLC-ESI-Q-TOF-MS to identify multiple constituents in processed products of the herbal medicine *Ligustri Lucidi Fructus*. Molecules 22 (5), 689.
- Liu, X., Zhang, J., Li, Y., Yao, C., An, Y., Wei, W., Yao, S., Yang, L., Huang, Y., Qu, H., Guo, D.A., 2022. In-depth profiling, nontargeted metabolomic and selective ion monitoring of eight chemical markers for simultaneous identification of different part of *Eucommia ulmoides* in 12 commercial products by UPLC/QDa. Food Chem. 393, 133346.
- Luo, M., Hou, F., Dong, L., Huang, F., Zhang, R., Su, D., 2020. Comparison of microwave and high-pressure processing on bound phenolic composition and antioxidant activities of sorghum hull. Int. J. Food Sci. Technol. 55 (9).
- Maleki, S.J., Crespo, J.F., Cabanillas, B., 2019. Anti-inflammatory effects of flavonoids. Food Chem. 299, 125124.
- Masek, A., Latos-Brozio, M., Kaluzna-Czaplińska, J., Rosiak, A., Chrzescijanska, E., 2020. Antioxidant properties of green coffee extract. Forests 11 (5), 557.
- Mena, P., Tassotti, M., Andreu, L., Nuncio-Jáuregui, N., Legua, P., Del Rio, D., Hernández, F., 2018. Phytochemical characterization of different prickly pear (*Opuntia ficus-indica* (L.) Mill.) cultivars and botanical parts: UHPLC-ESI-MS(n) metabolomics profiles and their chemometric analysis. Food Res. Int. 108, 301–308.
- Y. Niu, S. Wang, C. Li, et al. Effective compounds from *Caesalpinia sappan* L. on the tyrosinase in vitro and in vivo. Nat. Prod. Commun. 15 2020 1934578X20920055.
- Peixoto Araujo, N.M., Arruda, H.S., dos Santos, F.N., de Moraes, D.R., Pereira, G.A., Pastore, G.M., 2020. LC-MS/MS screening and identification of bioactive compounds in leaves, pulp and seed from *Eugenia calycina* Cambess. Food Res. Int. 137, 109556.
- Peralbo-Molina, Á., Priego-Capote, F., Luque de Castro, M.D., 2012. Tentative identification of phenolic compounds in olive pomace extracts using liquid chromatography-tandem mass spectrometry with a quadrupole-quadrupole-time-of-flight mass detector. J. Agric. Food Chem. 60 (46), 11542–11550.
- Sánchez-Salcedo, E.M., Tassotti, M., Del Rio, D., Hernández, F., Martínez, J.J., Mena, P., 2016. (Poly)phenolic fingerprint and chemometric analysis of white (*Morus alba* L.) and black (*Morus nigra* L.) mulberry leaves by using a non-targeted UHPLC-MS approach. Food Chem. 212, 250–255.
- Shi, S., Li, K., Peng, J., Li, J., Luo, L., Liu, M., Chen, Y., Xiang, Z., Xiong, P., Liu, L., 2022. Chemical characterization of extracts of leaves of *Kadsua coccinea* (Lem.) AC Sm. by UHPLC-Q-Exactive Orbitrap Mass spectrometry and assessment of their antioxidant and anti-inflammatory activities. Biomed. Pharmacother. 149, 112828.
- Sun, C., Liu, Y., Zhan, L., Rayat, G.R., Xiao, J., Jiang, H., Chen, K., 2021. Anti-diabetic effects of natural antioxidants from fruits. Trends Food Sci. Technol. 117, 3–14.
- S.N. Tang, J.B. Yang, S. E. S. He, J.X. Li, K.Q. Yu, M. Zhang, Q. Li, L. Sun, H. Li, 2022. Rapid Identification of Constituents in *Cephalanthus tetrandrus* (Roxb.) Ridsd. et Badh. F. Using UHPLC-Q-Exactive Orbitrap Mass Spectrometry. Molecules. 27(13): 4038.
- Vieira de Moraes, D., Rosalen, P.L., Ikegaki, M., de Souza Silva, A.P., Massarioli, A.P., de Alencar, S.M., 2021. Active antioxidant phenolics from Brazilian Red propolis: An optimization study for their recovery and identification by LC-ESI-QTOF-MS/MS. Antioxidants 10 (2), 297.
- Wang, S., Sun, X., An, S., Sang, F., Zhao, Y., Yu, Z., 2021. High-throughput identification of organic compounds from *Polygoni Multiflori Radix Praeparata* (Zhiheshouwu) by UHPLC-Q-Exactive Orbitrap-MS. Molecules 26 (13), 3977.
- Xu, Y., Xie, H., Chen, H., Xiong, L., Sa, K., Wang, X., Chen, L., 2022. Terpenoids and phenylpropanoids isolated from the twigs and leaves of *Abelia macrotera* and their anti-inflammatory activities. Chem. & Biodivers. 19 (12), e202200870.
- Yılmaz, M.A., Taslimi, P., Kılıç, Ö., et al., 2023. Unravelling the phenolic compound reserves, antioxidant and enzyme inhibitory activities of an endemic plant species, *Achillea Pseudoaleppica*. J. Biomol. Struct. Dyn. 41, 445–456.
- Yu, S., Liu, H., Li, K., Qin, Z., Qin, X., Zhu, P., Li, Z., 2019. Rapid characterization of the absorbed constituents in rat serum after oral administration and action mechanism of *Naozhenneng* granule using LC-MS and network pharmacology. J. Pharm. Biomed. Anal. 166, 281–290.
- Zeng, M.L., Shen, N.T., Wu, S.W., Li, Q., 2017. Analysis on chemical constituents in *Tetragium hemsleyanum* by UPLC-Triple-TOF/MS. J. Tradit. Chin. Med. 48 (05), 874–883.
- Zhang, Y., 2013. Preliminary studies on the physicochemical properties and physiological activity of *Abelia engleriana* leaf pectin. J. Northwest A&F Univ.
- Zhang, Y., Li, Y., Ren, X., Zhang, X., Wu, Z., Liu, L., 2023. The positive correlation of antioxidant activity and prebiotic effect about oat phenolic compounds. Food Chem. 402, 134231.
- Zong, S., Wang, H., Li, J., et al., 2021. Chemical compositions, anti-oxidant and anti-inflammatory potential of ethanol extract from *Zhuke-Hulu* tea. Food Biosci. 44, 101351.